

# Influence of Surface Segregation on Wetting of Sn-Ag-Cu (SAC) Series and Pb-Containing Solder Alloys

M.J. BOZACK,<sup>1,3</sup> J.C. SUHLING,<sup>2</sup> Y. ZHANG,<sup>2</sup> Z. CAI,<sup>2</sup> and P. LALL<sup>2</sup>

1.—Surface Science Laboratory, Department of Physics, Center for Advanced Vehicle and Extreme Environment Electronics (CAVE3), Auburn University, Auburn, AL 36849, USA. 2.—Department of Mechanical Engineering, Center for Advanced Vehicle and Extreme Environment Electronics (CAVE3), Auburn University, Auburn, AL 36849, USA. 3.—e-mail: bozack@physics.auburn.edu

Wetting of Sn-Ag-Cu (SAC) series solder alloys to solid substrates is strongly influenced by surface segregation of low-level bulk impurities in the alloys. We report *in situ* and real-time Auger electron spectroscopy measurements of SAC alloy surface compositions as a function of temperature as the alloys are taken through the melting point. A dramatic increase in the amount of surface C (and frequently O) is observed with temperature, and in some cases the alloy surface is nearly 80 at.% C at the melting point. The C originates from low-level impurities incorporated during alloy synthesis and inhibits wetting because C acts as a blocking layer to reaction between the alloy and substrate. A similar phenomenon has been observed over a wide range of (SAC and non-SAC) alloys synthesized by a variety of techniques. That solder alloy surfaces at melting have a radically different composition from the bulk uncovers a key variable that helps to explain the wide variability in contact angles reported in previous studies of wetting and adhesion.

**Key words:** Pb-free solder, wetting, tin-silver-copper (Sn-Ag-Cu), SAC, wetting, Auger electron spectroscopy (AES), surface segregation

## INTRODUCTION

The wetting of solid surfaces by liquid metals and alloys is important in several areas of technology and materials science. Liquid-phase sintering, detergency, adhesion, wear, catalysis, impregnation of porous materials by liquid binders, crystal growth from the melt, and solderability are largely determined by the ability of a liquid alloy to wet and spread over a solid. Despite the importance of interfacial surface chemistry involved in wetting, there have been comparatively few studies of liquid surfaces using surface analytical techniques, largely due to the risk involved when heating materials to melting inside expensive ultrahigh-vacuum systems. Hardy and Fine<sup>1</sup> noted in 1982 that they were aware of only two previous applications of Auger spectroscopy to the study of liquid surfaces. The

pioneering works were by Berglund and Somorjai,<sup>2</sup> who studied surface segregation in Pb-In alloys, and Goumiri and Joud,<sup>3</sup> who studied the influence of oxygen coverage on the surface tension and contact angle of Al-Sn alloys. The situation has changed little since that time.

In the case of electronic assembly, the wetting of solid board finishes by liquid solder alloys is a key reliability issue. The criteria for wetting and spreading of a liquid on an ideally flat, solid surface at equilibrium is given in terms of the Young–Dupré equation, which relates the liquid–vapor  $\gamma_{lv}$ , solid–vapor  $\gamma_{sv}$ , and solid–liquid  $\gamma_{sl}$  surface tensions to the wetting angle  $\theta$ :

$$\cos \theta = (\gamma_{sv} - \gamma_{sl}) / \gamma_{lv}. \quad (1)$$

This relation shows that, for good wetting, the surface tensions ( $\gamma_{sl}$  and  $\gamma_{lv}$ ) associated with the liquid phase should be low whereas the solid–vapor surface tension ( $\gamma_{sv}$ ) should be high. For wetting systems far from equilibrium,  $\gamma_{sl}$  is lowered

(Received January 20, 2011; accepted July 20, 2011; published online August 9, 2011)

primarily by dissolution and chemical reaction with the substrate;  $\gamma_{sv}$  is raised by having a clean solid surface, since adsorbed gases (unclean surface) lower the surface energy; and  $\gamma_{lv}$  can be lowered by gas adsorption or diffusion from the liquid bulk to the surface. For regular solutions, for example, it has been shown<sup>4</sup> that the lowering of  $\gamma_{sl}$  is related to the mole fraction  $X_s$  of solid dissolved in the liquid:

$$\gamma_{sl} = -RT(\ln X_s)/4A_m, \quad (2)$$

where  $A_m$  is the molar surface area of the liquid. A high degree of wettability will be exhibited by solder alloys which react strongly with and/or dissolve industry board finishes, which explains why Ni-Au finishes are such prolific wetting surfaces.

For spreading, it is desirable that  $\cos \theta = 1$ , or in terms of a spreading coefficient  $S$ ,

$$S = \gamma_{sv} - \gamma_{sl} - \gamma_{lv}, \quad (3)$$

where  $S > 0$ . Both wetting and spreading are favored by low values of the liquid surface tensions. One may also cast the Young–Dupré relationship in terms of the adhesion energy  $W_{ad}$  between the solid–liquid interface, where

$$W_{sd} = \gamma_{lv} + \gamma_{sv} - \gamma_{sl}. \quad (4)$$

From (1) and (4) one obtains

$$\cos \theta = W_{ad}/\gamma_{lv} - 1, \quad (5)$$

which means that spreading occurs when  $W_{ad} \geq 2\gamma_{lv}$ , where  $2\gamma_{lv}$  is the cohesion energy of the liquid. Spreading is favored when the adhesion between the liquid alloy and substrate is greater than the liquid alloy cohesion.

Applied studies of soldering are best performed in real time using surface analysis techniques and commercial board finishes rather than laboratory-created substrates. Previous solderability studies<sup>5</sup> in our laboratory and others have been conducted using one system for wetting but then another for AES/x-ray photoelectron spectroscopy (XPS) analysis. This is typically done due to limitations involved when heating a laminate-based board finish in an ultrahigh-vacuum (UHV) environment, which poses risks due to excessive substrate/solder outgassing during heating of the contact system to the melting point. We have recently overcome this difficulty and now do everything in one UHV surface analysis system without breaking vacuum or using cooling/reheating cycles.

We focus here on the wetting of SAC electronic solder alloys. In recent years, there has been a mandated shift from Sn-37Pb solder to emerging Pb-free solders in electronics applications. The shift has occurred due to political concerns about the health hazards of Pb in the electronics supply chain. The principal Pb-free solders currently under consideration are coined SAC alloys (e.g., SAC405 = 96.5Sn-4.0Ag-0.5Cu, etc.), which are ternary alloys containing the elements Sn, Ag, and Cu in various

mole fractions. While there have been considerable efforts<sup>6,7</sup> to elucidate the mechanical, thermal, and reliability properties of SAC alloys under isothermal, cycling, and field conditions, there has been comparatively little work on the wetting behavior. In the present effort, we report experiments using Auger electron spectroscopy (AES) which are designed to study the surfaces of SAC solder alloys under real-time, *in situ* conditions as the alloys are heated through the melting point. This is a primary factor in wetting, since the condition of the molten surface near and above the melting point affects the liquid–solid and liquid–vapor interfacial tensions and consequent ability of the alloy to react chemically with the joining solid surface. Our results show that the surface composition of the molten surface of SAC solder alloys is *radically different* from the surface composition at room temperature, with a direct and deleterious effect on wetting and spreading.

## EXPERIMENTAL PROCEDURES

Studies of the molten solder alloy surfaces were carried out in a Kratos XSAM 800 surface analysis system (Fig. 1). The base pressure of this load-locked, ion- and turbo-pumped system is  $7 \times 10^{-7}$  Pa as read on an uncalibrated, nude ion

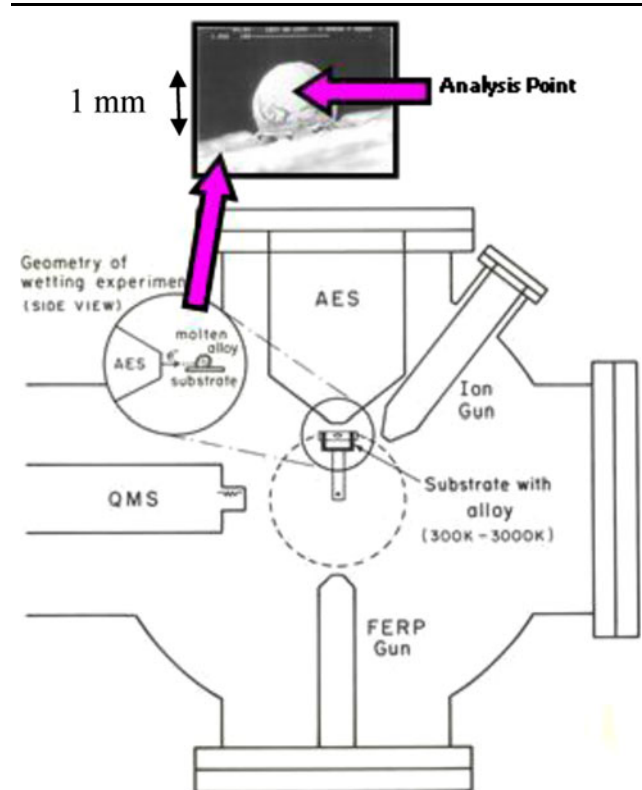


Fig. 1. Schematic diagram of the ultrahigh-vacuum section of the surface analytical system used for *in situ*, real-time AES liquid surface studies of SAC-based alloys.

gauge. The electron energy analyzer for the AES/XPS portion of the system is a 127-mm-radius double focusing concentric hemispherical energy analyzer (CHA) equipped with an aberration-compensated input lens (ACIL). AES spectra were recorded in fixed retard ratio (FRR) mode with retard ratio of 10. Such a retard ratio represents a compromise between sensitivity and resolution and is appropriate for acquisition of survey spectra. The AES energy axis was calibrated by setting the Cu (LMM) line to 914.4 eV referenced to the Fermi level.

To clean the starting alloy surfaces of adsorbed gases, light Ar<sup>+</sup>-ion sputter cleaning was accomplished by a differentially pumped Kratos Mini-beam I plasma discharge ion source with rastering and focusing capabilities. A variable scan voltage provides a high-frequency scan that yields a sputtered area of 1 cm<sup>2</sup> at the specimen position with a sputter rate of ~2.5 nm/min measured on a standard SiO<sub>2</sub> film. Auger spectra were taken on the solid and molten alloy surfaces from a focused spot (~0.1 mm) at a position near the center of the sputtered area. The angle of incidence of the ion beam with respect to the surface normal was 55°. All Auger spectra were recorded at 3.0 keV beam energy and 0.7 μA primary beam current, measured with applied +90 V bias. The detection system of the XSAM 800 consists of a single-channel multiplier and a fast-response head amplifier. Detector output modes include direct pulse counting and current detection with voltage-to-frequency (*V-F*) conversion. Due to the large exciting currents used, all spectra were recorded in *V-F* detection mode.

The raw Auger data were collected in *E·N(E)* integral mode by acquiring the spectrum of electrons emitted from the surface from energy of 50 eV to 600 eV, with starting energy of 50 eV to avoid collecting data from the intense, broad secondary-electron peak occurring in this energy region. For most SAC alloys, the atomic fraction of Ag and Cu is so small that the Auger spectrum is dominated by the triplet Sn (MNN) peaks from 320 eV to 440 eV. The low-weight-percent components Ag, having a principal (MNN) peak at 356 eV, and Cu, with a primary Cu (LMM) peak at 920 eV, are barely visible. Subsequently, the Savitsky-Golay<sup>8</sup> algorithm was employed to smooth the data and calculate the derivative Auger spectrum. Surface elemental compositions were determined by standard relative Auger sensitivity factors<sup>9</sup> supplied by the instrument manufacturer. It is the trend in relative Auger peak-to-peak heights during heating that is significant rather than the accuracy (~10% to 20%) of the surface composition numbers. Accurate stoichiometric calculations in AES are problematic due to the complex nature of Auger electron production, transmission, and detection.

The SAC alloys were eutectic or near-eutectic compositions of Sn-Ag-Cu synthesized commercially by Cookson Electronics<sup>10</sup> and supplied in bar form.

These alloys have narrow or zero pasty ranges with broad, low-melting (MP ≈ 220°C) compositions over which the alloys remain liquid. Eutectic Sn-37Pb (MP = 183°C) was carried along in the experimental matrix for comparison with a leaded solder alloy. While we report solely on commercial alloys, similar experiments in our laboratory on special SAC compositions and mixed formulation solder alloys (mixtures of Sn-37Pb and SAC305) gave similar results.<sup>11</sup> The wetting substrate was aluminum covered with a native aluminum oxide, verified by x-ray photoelectron spectroscopy (XPS). This selection was made because aluminum oxide has an extremely large and negative Gibbs free energy of formation,<sup>12</sup> which produces a high wetting contact angle for most contacting materials due to the lack of chemical reaction and interdiffusion on such a stable substrate. High rates of chemical reaction and low contact angles would tend to confuse the interpretation of the data due to substrate elements which may diffuse into the alloy. Our goal was to completely isolate the contact system from any outside elemental sources.

In a typical composition versus temperature experiment, the SAC alloy was laid atop the aluminum oxide substrate and introduced into the ultrahigh vacuum system. The alloy fragment was usually rectangular in shape (2 mm × 3 mm × 1 mm in height) and held in contact with the substrate by gravity. No solder flux was employed. After the base pressure was achieved ( $7 \times 10^{-7}$  Pa), the alloy surface was sputter cleaned and then heated in 50°C increments (1°C/s rate) until the alloy melted. The heating was accomplished inside the vacuum system by a high-resistivity heater element inserted into the bottom of the stainless-steel sample mount holding the aluminum oxide and alloy. The approximate temperature of the alloy was indicated by a thermocouple built into the heater element. The melting point was easily verified by simultaneous optical and scanning electron microscopy (SEM) observations of morphological changes in the alloy at melting (the XSAM 800 is a scanning Auger system) and by the pressure burst in the system at melting due to trapped gases in the alloy. For most of the data reported herein, the Auger beam was positioned near the top of the alloy fragment, although the beam position had to be altered occasionally as the alloy changed shape from rectangular to circular during melting. In nearly all cases, the contact angle of SAC alloys on aluminum oxide changed from 0° before heating to ~180° at melting. It took a few minutes at the melting point for the alloy to attain a spherical liquid shape due to the sluggish kinetics and alloy viscosity. In a few cases, the adhesive forces were so low that the spherical molten alloy droplet rolled off the aluminum oxide substrate and into the bottom of the vacuum chamber. Acquisition of each Auger spectra required about 20 min, during which time the alloy was maintained at the target temperature.

## RESULTS

### Alloy Surface Composition Versus Temperature

The surface composition as a function of temperature for SAC305 and SAC405 on aluminum oxide is shown in Figs. 2 and 3, respectively. The result is representative for all SAC series alloys (SAC105, SAC205, SAC305, and SAC405). An increase in the fraction of surface C and O (with accompanying decrease in Sn) is typically observed with increasing temperature. In most cases, the increase is from ~0 at.% C (sputter cleaned) to ~50 at.% to 70 at.% C at the alloy melting temperature, and the increase begins before reaching the melting point. Figures 2 and 3a plot the trend with temperature, while Figs. 2 and 3b display individual survey AES spectra at three temperatures. Clearly, the most distinctive feature during the annealing is the dramatic growth of the C (KLL) Auger peak at 272 eV. The appearance of low concentrations of other low-level alloy impurities such as S, Cl, Ca, and P are also observed, particularly as the alloy crosses the melting point. *In situ* optical and electron microscopy observations of the molten, poorly wetted droplet frequently showed evidence of second-phase material floating on the surface of the liquid alloy (Figs. 1, 5). Cooling the alloy back to room temperature did not reverse the surface composition. Figure 4 shows similar trends and conclusions for Sn-37Pb during heating to and above the melting point. We include these data to show that impurity segregation is not distinctive to SAC series alloys but occurs for a more general range of metal alloys.

Statistics plays a role when measuring the surface properties of liquid metal alloys, observed during repeated measurements on alloy fragments cut from the same bar of as-cast solder. The elemental trends seen in Figs. 2–4 are nearly always observed, but as the electron micrographs in Figs. 1 and 5 show, poorly wetted alloy droplet surfaces after heating are frequently inhomogeneous due to the shell of segregated carbon. Real-time observations of the molten droplets by low-power zoom optical microscopy during heating in the vacuum system revealed that parts of the C surface crust can dynamically migrate during the course of the measurements, bringing different portions under the AES beam, resulting in statistical compositional variations over repeated experiments (microscale plate tectonics). A good example is given in Fig. 5b, which shows the segregated C shell appearance (at room temperature) in low-power optical (white light) microscopy after wetting a mixed formulation solder alloy MIX 10–90 (10% Sn-37Pb + 90% SAC305 by weight) to a Ni-Au board finish (no flux applied) showing an area of the alloy surface with ~100% surface-segregated C content (poor wetting and high contact angle) and low C content (good wetting and low contact angle). The AES spectra

were recorded directly after wetting in the surface analysis system (no breaking of vacuum).

### Origin of the Surface Carbon

The most ideal experimental setup for studies of solder alloy surface composition versus temperature would involve levitating the alloy within an ultra-high-vacuum system during Auger analysis, which (barring adsorbed gas atoms) would guarantee alloy isolation from all outside sources of other elements. In lieu of this, wetting to aluminum oxide and the ability to sputter clean the alloy surface of adsorbed gases before heating proved to be essential features of the experiment. Since the alloy was completely isolated from outside sources of carbon and other elemental species, *the material observed at the alloy surfaces during heating could only originate from the alloy itself in the form of low-level surface-segregated impurities*. Similar behavior<sup>11</sup> has been found when SAC alloys are wetted (without flux) to more reactive, common board finishes [Ni-Au, Pd-Ni, Ag-Cu, hot air solder leveled (HASL), etc.].

Sanity-check calculations of surface enrichment lend support to the experimental observation of surface segregation in molten, spherical specimens of SAC alloys. If we assume a level of bulk alloy contamination just below the limit of detection of energy-dispersive x-ray (EDX) analysis (~0.02 wt.%) and assume the entire weight percent to aggregate to the surface of a spherical droplet of SAC alloy whose radius is 0.5 mm, the thickness of the carbon shell formed is ~100 nm. This shows it is feasible for the high concentrations of C to originate from impurity surface-segregated material. Emission spectroscopic analysis from a variety of commercial solder alloys shows that such levels of bulk carbon contamination are the rule rather than the exception. To verify the order of magnitude calculation, we measured the thickness of the surface carbon shell formed on several poorly wetted spheres of SAC/Sn-37Pb alloys by Auger depth profiling. The carbon shell was ~80 nm to 120 nm in thickness on most solder alloys.

## DISCUSSION

The primary goal of this work is to determine what a solid substrate sees during wetting of molten SAC solder alloys. Since the soldering process involves heating the solder to a temperature greater than the alloy melting point, the substrate sees the liquid surface above the melting point, not the solid surface at room temperature. If the solid and liquid surfaces are elementally different, presumptions made by flux chemists about what surface species exist on solder alloy surfaces will result in inefficient flux formulations. A secondary goal of this research was to determine whether the surface-segregation effects observed by one of us (M.J.B.) over 20 years ago in boride and arsenide alloys are



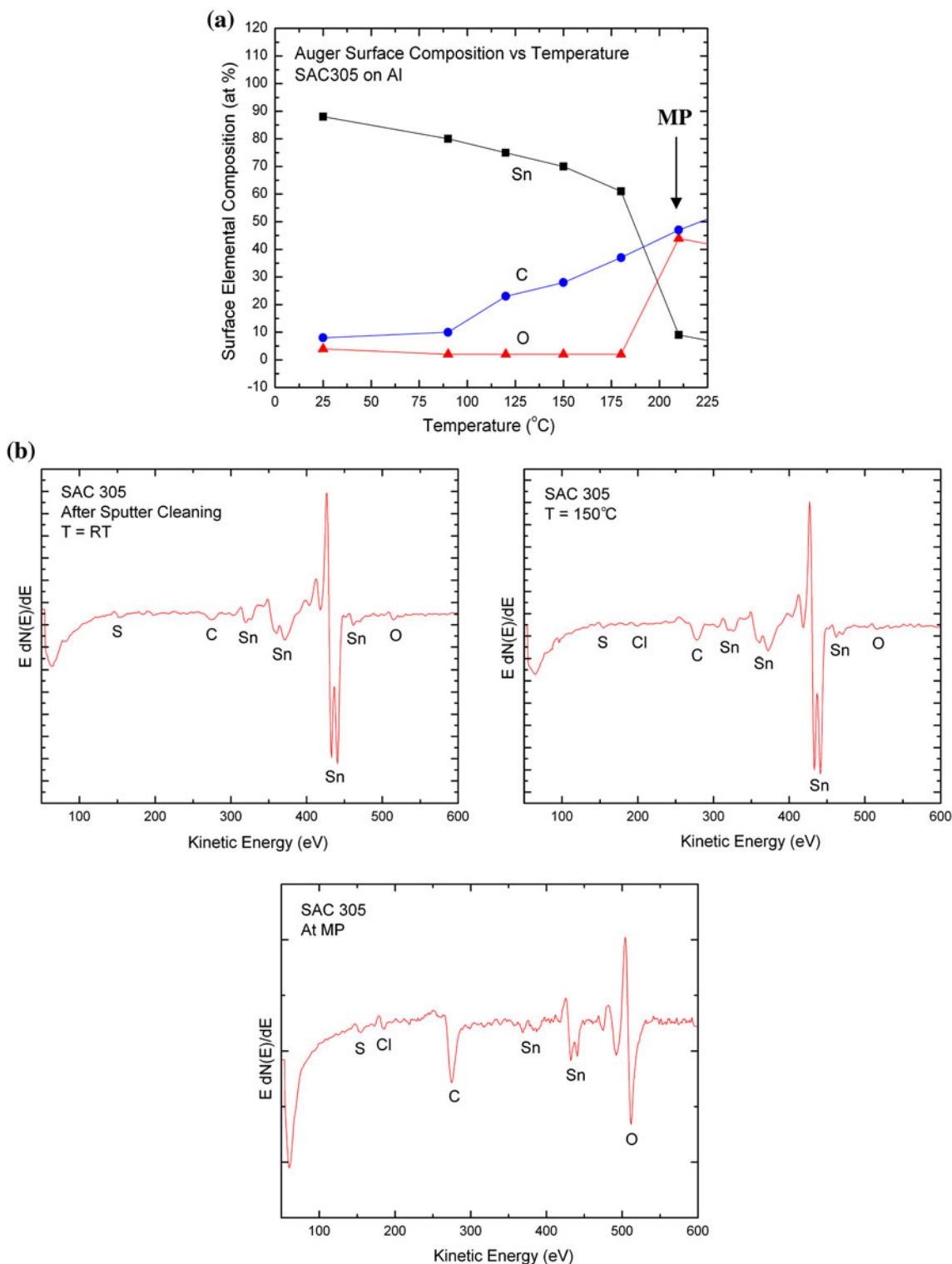


Fig. 2. (a) Auger surface elemental composition of SAC305 alloy versus temperature; (b) individual AES survey spectra for three temperatures (RT, 150°C, MP).

also exhibited in modern electronic solder alloys. The answer is yes.

Two decades ago, the context was to produce high-brightness, focused ion beams using liquid metal ion sources (LMIS), which are employed today as field-

ion sources in secondary-ion mass spectroscopy (SIMS) and focused ion beam (FIB) instrumentation. In a LMIS, a low-melting liquid such as gallium is required to wet a solid substrate without the assistance of flux, which would degrade the ion

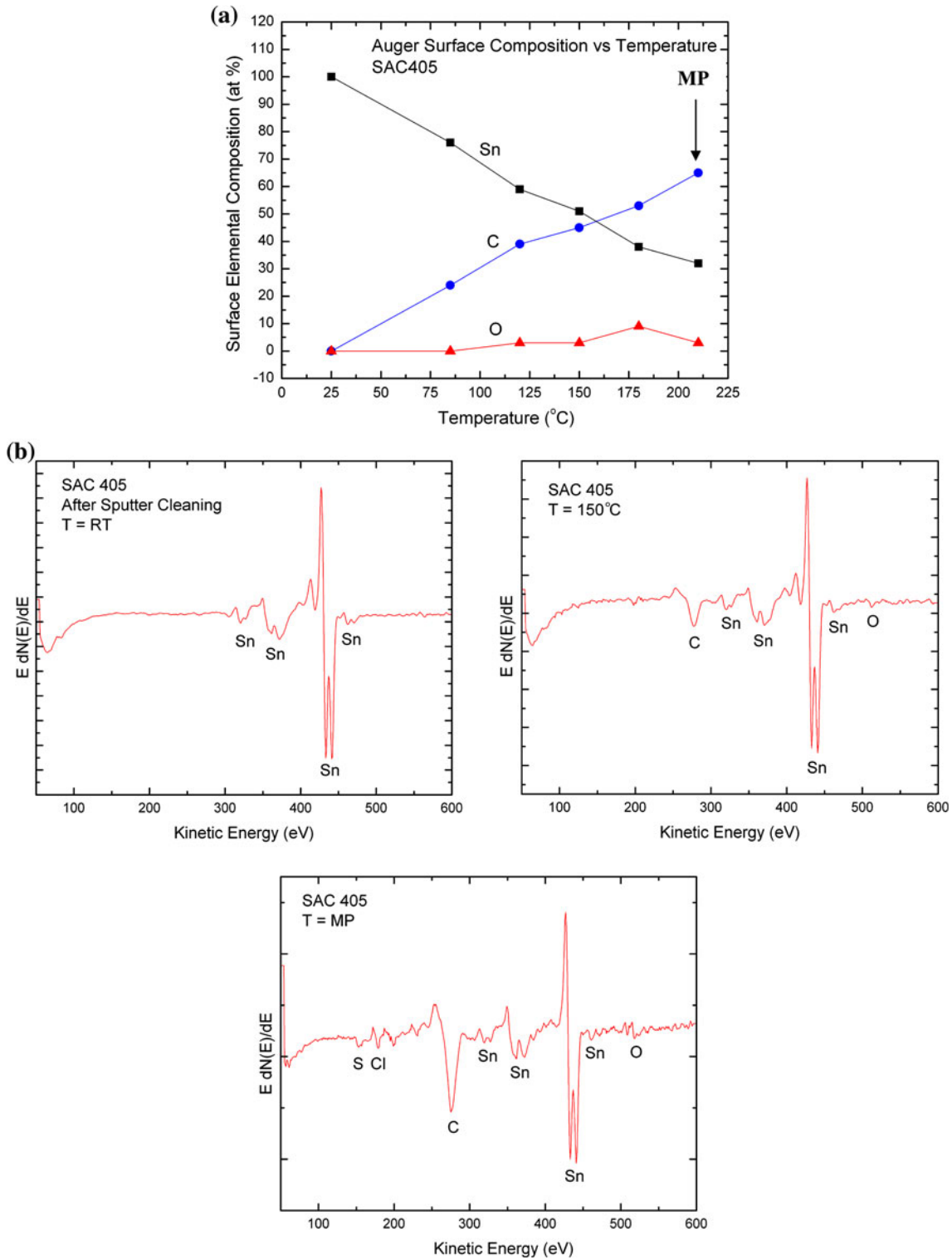


Fig. 3. (a) Auger surface elemental composition of SAC405 alloy versus temperature; (b) individual AES survey spectra for three temperatures (RT, 150°C, MP).

beam brightness and purity. At the time, we were studying boride and arsenide alloys in order to develop a LMIS of B and As for fine-focused dopant (B and As) ion implantation applications.<sup>13</sup> The boride and arsenide alloys were made by the

Materials Chemistry Group at Los Alamos National Laboratory by arc melting and combustion synthesis techniques, respectively. The greatest impediment to the development process was the inability of the alloys to wet compatible field-emission

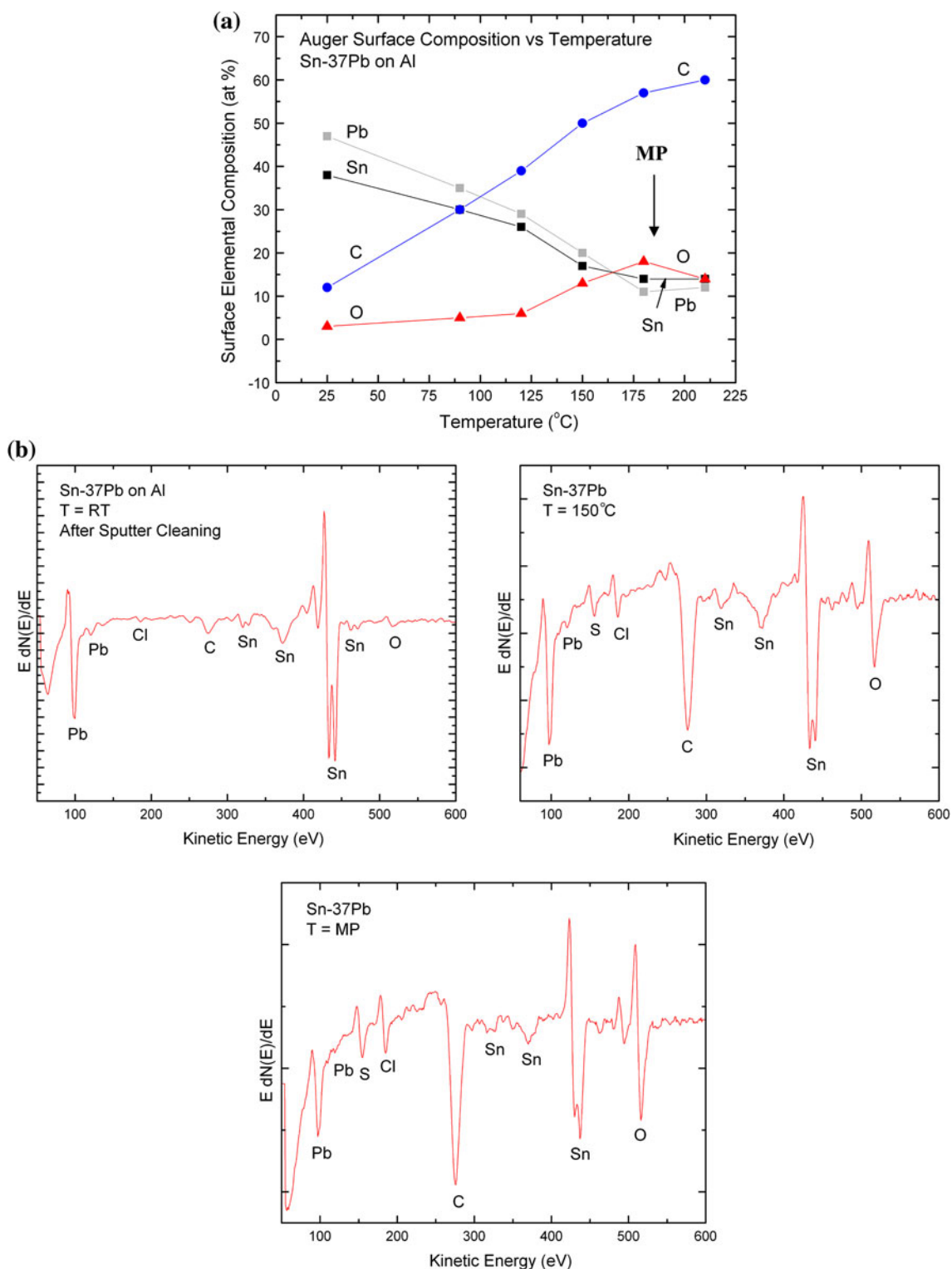


Fig. 4. (a) Auger surface elemental composition of Sn-37Pb alloy versus temperature; (b) individual AES survey spectra for three temperatures (RT, 150°C, MP).

substrates due to surface-segregated carbon originating from low-level impurities in the alloys, *precisely the same phenomenon* we have observed here for SAC and eutectic Sn-37Pb solder alloys.

It is likely that surface segregation of low-level bulk impurities is a ubiquitous phenomenon spanning a wide variety of alloys and alloy synthesis techniques. We have now observed it in boride

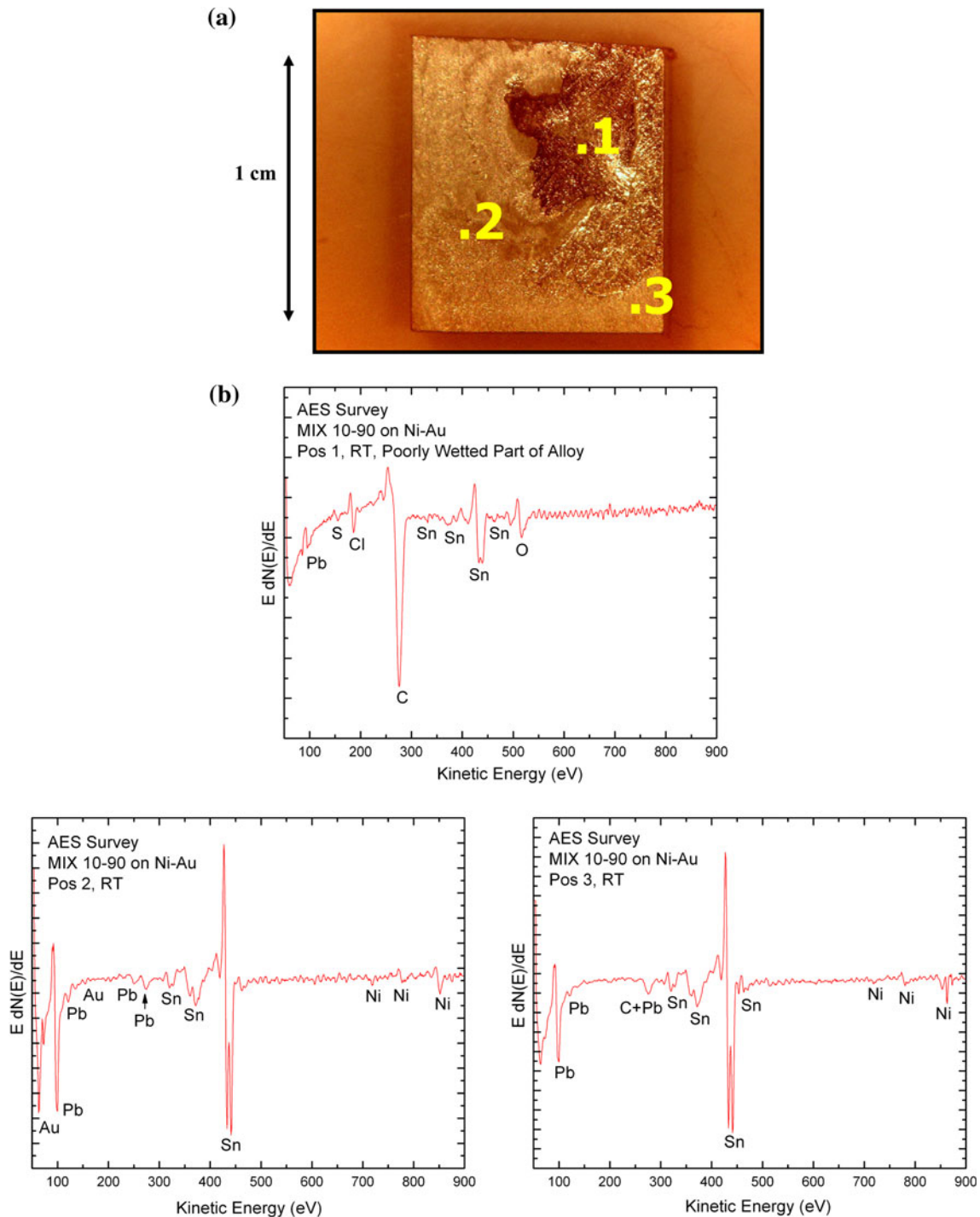


Fig. 5. Surface inhomogeneities after wetting. (a) Optical microscope photograph of mixed formulation alloy MIX 10-90 (10% Sn-37Pb + 90% SAC305 by weight) wetted to Ni-Au (no flux applied) after heating to  $>MP$  and subsequent cooling to room temperature. The numbers indicate AES analysis positions; (b) Auger spectra at positions 1-3 on the alloy after wetting, showing areas of the alloy surface with  $\sim 100\%$  surface-segregated C content (poor wetting and high contact angle) and low C content (good wetting and low contact angle). The AES spectra were recorded immediately after wetting in the surface analysis system.

alloys manufactured by the arc melting technique, arsenide alloys manufactured by the combustion synthesis technique, and solder alloys made by induction heating of the elemental metals in a variety of academic and commercial laboratories.

Surface analytical techniques are required to observe the segregated impurity layer, which is typically too thin ( $<100$  nm) to observe with standard SEM/EDX techniques, where the sampling volume is on the order of 2000 nm to 3000 nm



beneath the surface when using conventional accelerating voltages ( $\sim 20$  kV) employed by most investigators who do EDX analysis.

The widespread nature of impurity segregation occurs because it is difficult to synthesize high-purity alloys in conventional furnaces owing to effects traceable to poor chamber vacuum and impure starting materials. A typical arc melting apparatus, for example, operates under an inert gas atmosphere of at least hundreds of Pa in pressure with no provision for evacuation to high or ultrahigh vacuum. Common impurities such as nitrogen, oxygen, and carbon can readily get incorporated into the alloy bulk during synthesis, which can seriously degrade the results of subsequent materials studies. It is economically unfeasible to ensure sufficiently clean conditions during alloy synthesis to completely nullify the effects of surface segregation.

One method to exploit, rather than mitigate, the effects of impurity surface segregation<sup>14</sup> is to reheat the synthesized alloys, allow segregation to occur, and then skim or react off the impurity shell. It has been shown that, for many alloys, the interiors of poorly wetted droplets of alloy are pure to the detection limit ( $\sim 0.1$  wt.% or  $\sim 20$  ppm to 200 ppm)<sup>15</sup> of Auger and EDX spectroscopy. An example is seen in Fig. 5b, which shows that, in the case of wetting to a reactive substrate such as Ni-Au, there are regions where the wetting is excellent with little or no evidence of segregated carbon, while the C shell remnant is left behind at another part of the alloy.

The implications for technological applications which depend on the wetting of molten metal alloys are obvious; e.g., in the LMIS case, good wetting was eventually achieved by introducing boron into the contact system, which tied up the segregated carbon during formation of boron carbide.<sup>16</sup> Process engineers who deal with solderability, adhesion, and assembly issues should be aware that segregated impurities (rather than solely native oxides) may be the root cause of poor wetting and adhesion. The existence of surface segregation in molten liquids further calls into question many previous studies of wetting that were conducted blind without the advantage of surface analytical tools such as Auger spectroscopy.

There are several practical questions which emerge concerning impurity segregation. First, if impurity surface segregation is so prevalent in molten metal alloys, why do current solder alloys exhibit such high joint reliability? If an inert, impurity blocking layer exists on the surfaces of many molten solder materials, why does anything stick to them? The answer is twofold. In many highly reactive wetting systems (e.g., wetting to Ni-Au), the high rate of Au dissolution and strong chemical reaction with the substrate is sufficient to overcome the blocking effect of segregated carbon, which is often found to reside on the alloy surface as a cracked, inert mass of material. In our early

experiments (1988) on this issue, we were able to puncture the impurity shell by a sharp stylus within the vacuum chamber while the alloy was molten, which emitted pure alloy from the droplet interior which wet and spread beautifully on the substrate, the same substrate that initially formed a spherical ball. Further, modern solder pastes contain fluxes which clean the contacting surfaces of carbon as well as oxygen and other surface impurities. We know this is true due to wetting studies in our laboratory<sup>11</sup> and others involving organic solder preservative (OSP). Most solder pastes wet board finishes of OSP, which consists of a thin film of protective organic (carbon) covering Cu that protects it from oxidation and volatilizes during reflow. Thus, in the case of solder pastes, process engineers escape the more challenging problem of wetting in cases where flux usage is prohibited. It is indeed a fortuitous circumstance that the fluxes developed to clean the surfaces of native oxides also work to clean the segregated, impurity carbon.

Second, which segregated element (C or O) has the largest impact on wetting and spreading? Clearly, both elements are detrimental to good wetting, but, as noted above, flux chemists have presumed that surface oxygen in the form of native oxides is the major impediment to wetting. This supposition is due to the well-established fact that common joining surfaces wetted in air are always covered with a native oxide. While this is true, the data from surface science investigations show that surface carbon is at least as important and probably the biggest offender when considering the liquid-vapor and liquid-solid interfaces in Young's equation. We say this because: (1) while we often observe increases in *both* surface impurities C and O with temperature, it is often the case that the *growth* of the Auger C(KLL) peak is more pronounced than the growth of the O(KLL) peak; (2) eyeball comparisons of the raw peak-to-peak heights of the O (KLL) and C(KLL) peaks in Auger spectra give an overestimation of the absolute amount of O on the surface. The Auger elemental sensitivity factors of O (0.5) and C (0.18) at the 3.0 kV incident electron beam energy used in our experiments are nearly 3-to-1, which means that the Auger spectrometer is roughly three times more *sensitive* to O in comparison to C. Calculations of Auger surface elemental compositions, such as those in Figs. 2–4, take this factor into account; (3) controlled, *in situ* studies of wetting, such as reported in Fig. 5, characteristically show a better correlation between poor wetting and the amount of surface C (rather than surface O); and (4) experience in our surface laboratory and others over several years has shown that the major common surface impurity for the vast number of solid and liquid surfaces where adhesion is a problem contain a large fraction of surface C.

Third, what elements are likely to surface segregate and what is the driving force for surface

segregation? Is the observed temperature dependence predictable? Has impurity segregation been observed by other investigators? There are a number of theoretical models that involve surface segregation ranging from simple to complex and which address equilibrium and nonequilibrium situations. A brief discussion of two of the models provide the theory and intuitive insight to help explain impurity segregation in complex, nonideal, far-from-equilibrium materials involved with solder alloys.

Surface segregation is not a new phenomenon; indeed, Gibbs<sup>17</sup> developed a comprehensive thermodynamic formalism for it over a century ago. Experimental verifications of the Gibbs theory, however, awaited the development of surface-sensitive spectroscopies during the 1970s and the connection of the Gibbs formalism to quantities that are directly observable in surface experiments. The complex nature of multicomponent solder alloys poses a challenge for the theories of surface segregation, most of which are based on monolayer-scale segregation, ideal solutions, and ideal surfaces at equilibrium. Accordingly, there have been several attempts to develop Ising-like atomic statistical models, most of which have used a regular solution approximation.<sup>18</sup> The regular solution model allows for only two contributions to the free energy of the solution, an entropy contribution assumed to arise from the random distribution of atoms (ideal solutions) and an enthalpy-of-mixing contribution. The treatments address a system of two phases, a “bulk phase” and a “surface phase,” and consider a semi-infinite system consisting of a two-component solid. The common procedure minimizes the total free energy of the system with respect to the compositions of both phases. The general result can be written as

$$X_A^s/X_B^s = (X_A^b/X_B^b) \exp[-\Delta H_s/kT], \quad (6)$$

where  $X_A^s$ ,  $X_B^s$  ( $X_A^b$ , and  $X_B^b$ ) are the equilibrium atom fractions of components A and B in the surface (bulk) phases, respectively, for the two constituents, and  $\Delta H_s$  is the heat of segregation. The heat of segregation is the driving force for the segregation process and represents the enthalpy change which results when an atom of type A lying in the bulk phase exchanges positions with an atom of type B lying in the surface phase. Differences between the various theories of surface segregation lie in the form of the expression for  $\Delta H_s$ . We briefly discuss two forms of  $\Delta H_s$  given by the regular solution model.

The simplest monolayer ideal-solution model<sup>19</sup> of surface segregation shows that low-surface-tension elements are likely to surface segregate. The surface composition of an ideal binary solution is related to the bulk composition by

$$X_A^s/X_B^s = (X_A^b/X_B^b) \exp[(\gamma_B - \gamma_A)a/kT], \quad (7)$$

where  $a$  is the average surface area occupied per atom,  $\gamma_A$  and  $\gamma_B$  are the surface tensions of the pure

components A and B,  $k$  is the Boltzmann constant, and  $T$  is the temperature. If  $\gamma_A < \gamma_B$ , the surface fraction of component A will increase exponentially, resulting in marked surface segregation. It is clear that the constituent with the lower surface tension will have a higher concentration on the surface. This is intuitive since the surface tension is a measure of the force per unit length or energy per unit area required to produce a surface. The driving force for surface segregation in this model relates to the difference in the binding energies between the two metal atoms, A–B and the binding energies in the pure components, A–A and B–B. The change in binding energy gives rise to a change in the surface tension of the binary system compared with the surface tension for the pure constituents. Metal alloys are not ideal solutions, since they generally have some finite heat of mixing, which is ignored in the ideal-solution monolayer approach; further, the monolayer approximation strictly applies only to solids where all layers below the top monolayer have the bulk composition. While the ideal solution monolayer model shows that surface tension differences are a key driving force in segregation, it fails to work for impurity segregation by giving the wrong temperature dependence, showing that the surface excess concentration of the segregating constituent should *diminish* with increasing temperature.

Owing in part to the difficulties in measuring accurate surface tension values, standard compilations of surface tension are lacking or inadequate. For metals, however, there is excellent correlation between surface tension and the heat of sublimation  $\Delta H_{\text{subl}}$ , because both properties are related to creation of a unit area of surface. For semiconductors, semimetals, and insulators, most tabulated values in the literature show that the elements of lowest surface tension are nonmetals (e.g., C, N, O, F, P, Cl, S). Nonmetallic elements are frequently dubbed surface active since they are the elements commonly observed on “clean” (99.999% pure) metal surfaces by surface analytical techniques. Figures 2–5 show several of these nonmetals appearing on the surfaces of heated SAC alloys. Bulk contaminants, many of which are pinned in metal alloys at the grain boundaries, are released at melting when the boundaries disappear and the low-surface-tension components surface segregate in order to minimize the overall free energy of the system.

A second, more realistic regular solution model corrects the monolayer, ideal-solution model and shows that more solute should segregate with increasing temperature. This was demonstrated by Lea and Seah,<sup>20</sup> who developed a model for surface segregation based on a solution of the diffusion equation by McLean<sup>21</sup> for the case of grain boundary segregation. The general solution can be written

$$\frac{X^s(t)}{X^s(\infty)} = 1 - \exp\left(\frac{D \cdot t}{\alpha^2 \cdot d^2}\right) \operatorname{erfc}\left(\frac{D \cdot t}{\alpha^2 \cdot d^2}\right)^{1/2}, \quad (8)$$

where  $X^s(t)$  and  $X^s(\infty)$  are the surface atom fractions of the segregating component at times  $t$  and  $\infty$ , respectively (i.e.,  $X^s(\infty)$  is the equilibrium atom fraction of the segregating component),  $\alpha$  is the ratio at equilibrium of the surface atom fraction to the bulk atom fraction,  $D$  is the bulk diffusion coefficient of the segregant through the alloy,  $d$  is the “thickness” of the segregated surface region (assumed to be one monolayer), and  $t$  is the time. In this model, bulk diffusion is the rate-determining step for surface segregation. Furthermore, local equilibrium is assumed between the surface and the nearby bulk region, which is described by the linear relation  $X^s(\infty) = \alpha \cdot X^b(\infty)$ , where  $X^b(\infty)$  is the solute concentration of the segregant and  $\alpha$  is called the enrichment factor. Equation (8) is strictly valid for low surface coverage because  $\alpha$  is assumed to be independent of  $X^s$ , which is not true for high surface concentrations near saturation. By expanding using a power series in  $P = \left(\frac{D \cdot t}{\alpha^2 \cdot d^2}\right)^{1/2}$  for small  $P$  values, higher-order terms can be neglected to give

$$\frac{X^s(t)}{X^s(\infty)} = \frac{2}{\sqrt{\pi}} \left(\frac{D \cdot t}{\alpha^2 \cdot d^2}\right)^{1/2}, \quad (9)$$

and by introducing the relation  $X^s(\infty) = \alpha \cdot X^b(\infty)$  one obtains

$$X^s(t) = [2/d\sqrt{\pi}](X^b)[\sqrt{(Dt)}], \quad (10)$$

where  $X^s(t)$  is the surface solute concentration at time  $t$ ,  $X^b$  is the solute concentration in the bulk,  $d$  is the thickness of a monolayer of segregant, and  $D$  is the effective diffusion coefficient. This shows that the free solute concentration in the bulk and the temperature are the primary factors controlling solute accumulation at the surface. Since the general form of the diffusion coefficient is  $D \sim D_0 \exp(-E_A/RT) \text{ m}^2/\text{s}$ , where  $D_0$  is the diffusion coefficient at infinite temperature and  $E_A$  is the activation energy, there is an exponential dependence of  $D$  on  $T$ . For a fixed hold time  $t$  at any temperature  $T$ , the element under consideration should show pronounced enrichment on the surface upon heating. The Lea–Seah formalism has been applied to a few solid surfaces and appears to give reasonable agreement with diffusion coefficients measured by tracer diffusion methods.<sup>22</sup> While it is hazardous to apply the theory to complex, nonideal, liquid solder alloys far from equilibrium, it is nevertheless useful to see the roles of temperature and time on segregation.

Impurity segregation has been observed since the infancy of experimental surface science. In their 1979 paper, Wynblatt and Ku<sup>23</sup> report that surface segregation experiments had been done on a dozen or so binary alloy systems at that time. Impurity segregation, where C, O, Ca, S, and other nonmetals repeatedly appeared on the surfaces of the alloys, was considered to be a nuisance in the early experiments, whose goal was to examine monolayer-

scale segregation. Removal of these strongly segregating contaminants (usually by repeated sputter/heating cycles or reaction with oxygen) was important before starting the “true” segregation experiment involving the binary alloy components. This was because the impurities could interact preferentially with one or the other of the binary alloy elements and either enhance or suppress the natural segregating tendency of the uncontaminated alloy. In fact, Wynblatt and Ku<sup>24</sup> remark that “these species arise from strongly segregating tramp impurities present in the bulk alloy in trace quantities, and they can sometimes prove very difficult to remove.” Clearly, the significance of impurity segregation in metal alloys was recognized early in the development of modern surface science.

## CONCLUSIONS

Wetting of SAC series solder alloys to board finishes is directly influenced by surface segregation of low-level bulk alloy impurities. The major segregating impurities are C and O at the molten solder alloy surface. The impurity segregation is not temperature reversible.

The impurities form a high-surface-tension shell around the alloy and inhibit chemical reaction with the substrate, resulting in poor wettability. The interior of poorly wetted droplets of alloy is composed of pure alloy material which allows for varying amounts of good wetting and spreading depending on the contacting materials. Wetting is sluggish in locations where the carbon shell remnant is located.

Impurity surface segregation has been observed over a wide range of alloys synthesized by a variety of different alloy manufacturing techniques. Solder fluxing remedies the problem with impurity segregation by cleaning both carbon and oxygen from surfaces. The clear message from this work is that surface analytical tools are essential for studies of wetting and adhesion.

## ACKNOWLEDGEMENTS

We gratefully acknowledge the industrial members of the Center for Advanced Vehicle Electronics and Extreme Environment Electronics (CAVE3) for continued support of this work.

## REFERENCES

1. S. Hardy and J. Fine, *Materials Processing in the Reduced Gravity Environment of Space*, ed. G.E. Rindone (Amsterdam: Elsevier, 1982), p. 503.
2. S. Berglund and G.A. Somorjai, *J. Chem. Phys.* 59, 5537 (1973).
3. L. Goumiri and J.C. Joud, *Acta Metall.* 30, 1397 (1982).
4. Ju.V. Naidich, *Prog. Surf. Membr. Sci.* 14, 353 (1981).
5. S.V. Sattiraju, B. Dang, R.W. Johnson, Y. Li, J.S. Smith, and M.J. Bozack, *IEEE Trans. Electron. Packag. Manuf.* 25, 168 (2002).
6. H. Ma, J.C. Suhling, P. Lall, and M.J. Bozack, *Proc. 56th Electronic Components and Technology Conference*, 2006, p. 16ff.

7. Y. Zhang, Z. Cai, J.C. Suhling, P. Lall, and M.J. Bozack, *Proc. 58th IEEE Electronic Components and Technology Conference*, Orlando, FL, May 28–30, 2008, pp. 99–112.
8. A. Savitzky and M. Golay, *Anal. Chem.* 36, 1627 (1964).
9. P.W. Palmberg, G.E. Riach, R.E. Weber, and N.C. MacDonald, *Handbook of Auger Electron Spectroscopy* (Edina, MN: Physical Electronics Industries, 1972).
10. Cookson Electronics Assembly Materials, South Plainfield, NJ.
11. M.J. Bozack, J.C. Suhling, Y. Zhang, Z. Cai, and P. Lall, *J. Vac. Sci. Technol. A* 29 (4), 041401 (2011).
12. C.E. Wicks and F.E. Block, *Thermodynamic Properties of 65 Elements—Their Oxides, Halides, Carbides, and Nitrides* (Washington, DC: Bureau of Mines Bulletin 605, U.S. Government Printing Office, 1963).
13. M.J. Bozack, L.W. Swanson, and A.E. Bell, *J. Mater. Sci.* 22, 2421 (1987).
14. M.J. Bozack and P.R. Davis, *Mater. Sci. Eng. A* 150, 255 (1992).
15. P. Kuisma-Kursula, *X-ray Spectrom.* 29, 111 (2000).
16. M.J. Bozack, A.E. Bell, and L.W. Swanson, *J. Phys. Chem.* 92, 3925 (1988).
17. J.W. Gibbs, *The Scientific Papers of J. Willard Gibbs*, Vol. 1 (New York: Dover, 1961), p. 219.
18. W.C. Johnson and J.M. Blakely, eds., *Interfacial Segregation* (Metals Park, OH: American Society for Metals, 1979).
19. G.A. Somorjai, *Introduction to Surface Chemistry and Catalysis* (New York: Wiley, 1994), p. 285ff.
20. C. Lea and M.P. Seah, *Philos. Mag.* 35, 213 (1977).
21. D. McLean in, *Grain Boundaries in Metals* (Oxford: Clarendon, 1957).
22. K. Hennesen, H. Keller, and H. Viefhaus, *Scripta Metall.* 18, 1319 (1984).
23. P. Wynblatt and R.C. Ku, *Interfacial Segregation*, ed. W.C. Johnson and J.M. Blakely (Metals Park, OH: American Society for Metals, 1979), p. 127.
24. P. Wynblatt and R.C. Ku, *Interfacial Segregation*, ed. W.C. Johnson and J.M. Blakely (Metals Park, OH: American Society for Metals, 1979), p. 117.